REAM intensity modulator-enabled 10Gb/s colorless upstream transmission of real-time optical OFDM signals in a single-fiber-based bidirectional PON architecture

E. Hugues-Salas,[1,*] R. P. Giddings,[1] X. Q. Jin,[1] Y. Hong,[1] T. Quinlan,[2] S. Walker,[2] and J. M. Tang[1]

[1]*School of Electronic Engineering, Bangor University, Dean Street, Bangor, LL57 1UT, UK*
[2]*School of Computer Science and Electronic Engineering, University of Essex, Colchester, CO43SQ, UK*
[*]*e.hugues-salas@bangor.ac.uk*

Abstract: Reflective electro-absorption modulation-intensity modulators (REAM-IMs) are utilized, for the first time, to experimentally demonstrate colorless ONUs in single-fiber-based, bidirectional, intensity-modulation and direct-detection (IMDD), optical OFDM PONs (OOFDM-PONs) incorporating 25km SSMFs and OLT-side-seeded CW optical signals. The colorlessness of the REAM-IMs is characterized, based on which optimum REAM-IM operating conditions are identified. In the aforementioned PON architecture, 10Gb/s colorless upstream transmissions of end-to-end real-time OOFDM signals are successfully achieved for various wavelengths within the entire C-band. Over such a wavelength window, corresponding minimum received optical powers at the FEC limit vary in a range as small as <0.5dB. In addition, experimental measurements also indicate that Rayleigh backscattering imposes a 2.8dB optical power penalty on the 10Gb/s over 25km upstream OOFDM signal transmission. Furthermore, making use of on-line adaptive bit and power loading, a linear trade-off between aggregated signal line rate and optical power budget is observed, which shows that, for the present PON system, a 10% reduction in signal line rate can improve the optical power budget by 2.6dB.

©2012 Optical Society of America

OCIS codes: (060.0060) Fiber optics and optical communications; (060.2340) Fiber optics components; (060.4080) Modulation.

References and links

1. N. Yoshimoto, "The role of advanced EPON systems and their related technologies for sustainable growth of telecom industry," in Proceedings of Asia Communications and Photonics Conference (ACP), (Shanghai, China, 2010).
2. J. Kani, "Enabling technologies for future scalable and flexible WDM-PON and WDM/TDM-PON systems," IEEE J. Sel. Top. Quantum Electron. **16**(5), 1290–1297 (2010).
3. S. Kaneko, Jun-ichi Kani, K. Iwatsuki, A. Ohki, M. Sugo, and S. Kamei, "Scalability of spectrum-sliced DWDM transmission and its expansion using forward error correction," J. Lightwave Technol. **24**(3), 1295–1301 (2006).
4. F. Raharimanitra, P. Chanclou, T. N. Duong, J. Le Masson, B. Charbonnier, M. Ouzzif, N. Genay, A. Gharba, F. Saliou, R. Brenot, and G. Devalicourt, "Spectrum sliced sources AMOOFDM modulated for WDM&TDM PON," European Conference on Optical Communication (ECOC), (Vienna, 2009), Paper 6.5.3.
5. H. Suzuki, M. Fujiwara, T. Suzuki, N. Yoshimoto, H. Kimura, and M. Tsubokawa, "Wavelength-tunable DWDM-SFP transceiver with a signal monitoring interface and its application to coexistence-type colorless WDM-PON," European Conference on Optical Communication (ECOC), (Berlin, 2007), Paper PD3.4.
6. R. Urata, C. Lam, H. Liu, and C. Johnson, "High performance, low cost, colorless ONU for WDM-PON," Optical Fiber Communication/National Fiber Optic Engineers Conference (OFC/NFOEC), (USA, 2012), Paper Nth3E.4.
7. N. Genay, P. Chanclou, R. Brenot, M. Moignard, and F. Payoux, "Colourless ONU modules in TDM-PON and WDM-PON architectures for optical carrier remote modulation," European Conference on Optical Communication (ECOC), (Glasgow, 2005), Paper Tu1.3.6.
8. C. W. Chow, C. H. Yeh, C. H. Wang, F. Y. Shih, and S. Chi, "Signal remodulation of OFDM-QAM for long reach carrier distributed passive optical networks," IEEE Photon. Technol. Lett. **21**(11), 715–717 (2009).

9. R. P. Giddings, E. Hugues-Salas, X. Q. Jin, J. L. Wei, and J. M. Tang, "Experimental demonstration of real-time optical OFDM transmission at 7.5 Gb/s over 25-km SSMF using a 1-GHz RSOA," IEEE Photon. Technol. Lett. **22**(11), 745–747 (2010).
10. X. Q. Jin and J. M. Tang, "Experimental investigations of wavelength spacing and colorlessness of RSOA-based ONUs in real-time optical OFDMA PONs," J. Lightwave Technol. **30**(16), 2603–2609 (2012).
11. T. Duong, N. Genay, P. Chanclou, B. Charbonnier, A. Pizzinat, and R. Brenot, "Experimental demonstration of 10 Gbit/s upstream transmission by remote modulation of 1 GHz RSOA using adaptively modulated optical OFDM for WDM-PON single fiber architecture," European Conference on Optical Communication (ECOC), (Brussels, 2008), Paper Th.3.F.1.
12. A. Borghesani, "Reflective based active semiconductor components for next generation optical access networks," European Conference on Optical Communication (ECOC), (Torino, 2010), Paper Mo.1.B.1.
13. S. C. Lin, S. L. Lee, C. K. Liu, C. L. Yang, S. C. Ko, T. W. Liaw, and G. Keiser, "Design and demonstration of REAM-based WDM-PONs with remote amplification and channel fault monitoring," J. Opt. Commun. Netw. **4**(4), 336–343 (2012).
14. P. Ossieur, C. Antony, A. M. Clarke, A. Naughton, H. G. Krimmel, Y. Chang, C. Ford, A. Borghesani, D. G. Moodie, A. Poustie, R. Wyatt, B. Harmon, I. Lealman, G. Maxwell, D. Rogers, D. W. Smith, D. Nesset, R. P. Davey, and P. D. Townsend, "A 135-km 8192-split carrier distributed DWDM-TDMA PON with 2x32 10Gb/s capacity," J. Lightwave Technol. **29**(4), 463–474 (2011).
15. D. J. Shin, D. K. Jung, H. S. Shin, J. W. Kwon, S. Hwang, Y. Oh, and C. Shim, "Hybrid WDM/TDM-PON with Wavelength-selection-free transmitters," J. Lightwave Technol. **23**(1), 187–195 (2005).
16. C. H. Lee, "WDM-PON overview," European Conference on Optical Communication (ECOC), (Vienna, 2009), Paper 5.7.1.
17. Z. Xu, Y. Yeo, X. Cheng, and E. Kurniawan, "20-Gb/s injection locked FP-LD in a wavelength-division-multiplexing OFDM-PON," Optical Fiber Communication/National Fiber Optic Engineers Conference (OFC/NFOEC), (USA, 2012), Paper OW4B.3.
18. R. P. Giddings, X. Q. Jin, E. Hugues-Salas, E. Giacoumidis, J. L. Wei, and J. M. Tang, "Experimental demonstration of a record high 11.25Gb/s real-time optical OFDM transceiver supporting 25km SMF end-to-end transmission in simple IMDD systems," Opt. Express **18**(6), 5541–5555 (2010).
19. E. Hugues-Salas, R. P. Giddings, X. Q. Jin, J. L. Wei, X. Zheng, Y. Hong, C. Shu, and J. M. Tang, "Real-time experimental demonstration of low-cost VCSEL intensity-modulated 11.25 Gb/s optical OFDM signal transmission over 25 km PON systems," Opt. Express **19**(4), 2979–2988 (2011).
20. R. P. Giddings, E. Hugues-Salas, and J. M. Tang, "Experimental demonstration of record high 19.125Gb/s real-time end-to-end dual-band optical OFDM transmission over 25km SMF in a simple EML-based IMDD system," Opt. Express (accepted for publication).
21. E. Hugues-Salas, R. P. Giddings, X. Q. Jin, T. Quinlan, Y. Hong, S. Walker, and J. M. Tang, "REAM intensity modulator–enabled colorless transmission of real-time optical OFDM signals for WDM-PONs," to be presented at the European Conference on Optical Communication (ECOC), Amsterdam, The Netherlands, 16–20 Sept. 2012.
22. E. Hugues-Salas, X. Q. Jin, R. P. Giddings, Y. Hong, S. Mansoor, A. Villafranca, and J. M. Tang, "Directly modulated VCSEL-based real-time 11.25-Gb/s optical OFDM transmission over 2000-m legacy MMFs," IEEE Photon. J. **4**(1), 143–154 (2012).
23. X. Q. Jin, J. L. Wei, R. P. Giddings, T. Quinlan, S. Walker, and J. M. Tang, "Experimental demonstrations and extensive comparisons of end-to-end real-time optical OFDM transceivers with adaptive bit and/or power loading," IEEE Photon. J. **3**(3), 500–511 (2011).
24. J. L. Wei, E. Hugues-Salas, R. P. Giddings, X. Q. Jin, X. Zheng, S. Mansoor, and J. M. Tang, "Wavelength reused bidirectional transmission of adaptively modulated optical OFDM signals in WDM-PONs incorporating SOA and RSOA intensity modulators," Opt. Express **18**(10), 9791–9808 (2010).
25. E. Lach, K. Schuh, and M. Schmidt, "Application of electro-absorption modulators for high-speed transmission systems," J. Opt. Fiber. Commun. **2**(2), 140–170 (2005).
26. J. L. Wei, C. Sánchez, E. Hugues-Salas, P. S. Spencer, and J. M. Tang, "Wavelength-offset filtering in optical OFDM IMDD systems using directly modulated DFB lasers," J. Lightwave Technol. **29**(18), 2861–2870 (2011).

1. Introduction

Passive optical networks (PONs) are foreseen as the main technology in worldwide fiber-to-the-home (FTTH) deployments. The total number of global FTTH subscribers is projected to reach 100 million by 2013 [1]. To satisfy the explosive end-users' bandwidth requirement, wavelength-division-multiplexed PONs (WDM-PONs) are one of the most promising solutions for future mass deployment of next generation PONs (NG-PONs), since WDM-PONs offer significantly improved signal transmission capacity, enhanced system flexibility and wavelength scalability, virtual point-to-point connection enabling each individual end-user to be granted a single wavelength, protocol transparency and excellent network security [2]. To practically deploy WDM-PONs, the main challenges are cost-effectiveness and colorlessness of optical network units (ONUs). To address such challenges, several techniques have been proposed, which include, for example, spectrum-slicing of super luminescent

diodes (SLDs) or optical amplifiers [3,4], wavelength tunable lasers in ONUs [5,6] and remote modulation of reflective intensity modulators [7,8]. Among all these proposed techniques, reflective intensity modulation-based ONUs are very attractive for WDM-PONs since the implementation of a centrally-controlled dynamic wavelength management in an optical line terminal (OLT) allows the reflected upstream signal transmission from the ONU in a wavelength agnostic manner. Most importantly, since ONU-side laser sources are not present, the ONU transceiver complexity is greatly simplified and consequently the overall WDM-PON installation cost is significantly reduced by a factor proportional to the total number ONUs accommodated simultaneously in the network. To achieve reflective intensity modulation-based cost-effective ONUs, the following reflective intensity modulators may be utilized, including, for example, reflective semiconductor optical amplifiers (RSOAs) [9–11], reflective electro-absorption modulators (REAMs) [12–14] and reflective Fabry-Perot lasers [15–17].

To further enhance signal transmission capacities of reflective WDM-PONs while still preserving their compatibility with existing time-division-multiplexing PONs (TDM-PONs), optical orthogonal frequency division multiplexing (OOFDM) has been considered as one of the strongest physical layer technologies, since OOFDM has inherent and unique advantages such as potential of providing cost-effective technical solutions by fully exploiting the rapid advances in modern digital signal processing (DSP) technology, dynamic provision of hybrid bandwidth allocation in the frequency and time domains, reduction in optical network complexity owing to its great resistance to dispersion impairments and efficient utilization of channel spectral characteristics. It is, therefore, preferable if use is made of OOFDM in reflective intensity modulator-based ONUs in WDM-PONs incorporating standard single mode fiber (SSMF) systems utilizing simple intensity modulation and direct detection (IMDD).

Recently, by making use of various commercially available, low-cost intensity modulators such as directly modulated distributed feedback (DFB) lasers [18] and vertical cavity surface-emitting lasers (VCSELs) [19], we have experimentally demonstrated end-to-end real-time 11.25Gb/s OOFDM transmission over 25km SSMF-based PON systems employing IMDD. In a very similar IMDD transmission system architecture, record high 19.125Gb/s end-to-end real-time dual-band OOFDM signal transmissions over 25km SSMFs have also been experimentally achieved recently [20], utilizing low-cost components including an electro-absorption modulated laser-based intensity modulator, a 4GS/s digital-to-analogue converter (DAC), as well as a 4GS/s analogue-to-digital converter (ADC). Moreover, end-to-end real-time colorless transmissions of 16-QAM- and 32-QAM-encoded OOFDM signals have also been reported in IMDD SSMF PON systems employing 1.125GHz RSOA intensity modulators (RSOA-IMs) [9,10]. To further improve the real-time colorless OOFDM transmission capacity, the use of REAM-intensity modulators (REAM-IMs) is greatly beneficial due to their intrinsic advantages such as relatively high modulation bandwidth, low driving current, reduced form factor and low power consumption [12,13]. Very recently, we have reported experimental demonstrations of REAM-IM-based colorless OOFDM-PON systems [21].

In this paper, the experimental investigations published in [21] are significantly extended due to the inclusion of a bidirectional, real-time, colorless, REAM-IM-based, IMDD OOFDM-PON operating at 10Gb/s over 25km SSMFs. Since the upstream transmission is more challenging compared to the corresponding downstream transmission, the main focus of the present paper is, therefore, to experimentally explore the maximum achievable upstream transmission performance of the aforementioned PON architecture. The colorlessness operation of the REAM-IM over the entire C-band is first characterized in a unidirectional PON system and optimum REAM-IM operating conditions are identified. Subsequently, we experimentally demonstrate, for the first time, 10Gb/s end-to-end real-time colorless upstream OOFDM transmission over single-fiber-based, bidirectional 25km SSMF IMDD PONs. As the upstream OOFDM signal transmission performance is considerably affected by the Rayleigh backscattering (RB) effect, the impact of the RB effect is also experimentally

investigated on the upstream OOFDM transmission performance. Finally, based on the adaptive bit and power loading function implemented in the real-time OOFDM transceivers, the dependence of the aggregated upstream signal transmission capacity on the minimum received optical power (ROP) at the FEC limit is experimentally explored in the bidirectional PON architecture of interest of the present paper.

2. Colorlessness characterization of REAM-IMs

2.1. REAM-IM-based OOFDM transceiver and experimental system setup

To identify the optimum REAM-IM operating conditions for colorless transmission of end-to-end real-time OOFDM signals within the entire C-band, in this section, the operating condition-dependent colorlessness of the REAM-IM is first characterized in a simple unidirectional, 25km SSMF, IMDD PON system. The considered experimental system setup is illustrated in Fig. 1. The OOFDM transceiver incorporates a 4GS/s @ 8-bit DAC, a 4GS/s @ 8-bit ADC and field programmable gate arrays (FPGAs) for performing real-time high-speed DSP. Full descriptions of all DSP algorithms and their key parameters are presented in [22,23]. The core FPGA-based DSP algorithms in the transmitter include pseudo-random test data generation, pilot-tone insertion, online adaptive bit and power loading for 15 data-carrying subcarriers at 125MHz spacing with signal modulation formats selected from 16-quaternatry amplitude modulation (QAM), 32-QAM and 64-QAM, 32-point inverse fast Fourier transform (IFFT) to generate real-valued time-domain OFDM symbols at 100MHz, on-line adaptive clipping, 8-bit sample quantization and addition of a 25% cyclic prefix. Apart from DSP algorithms performing functions inverse to their transmitter counterparts mentioned above, receiver DSP functions also include detection of pilot-subcarriers, automatic symbol synchronization and channel estimation/equalization. In addition, the OOFDM transceiver design also offers unique capabilities of online performance monitoring of total channel bit error rate (BER), subcarrier BER distribution and system frequency response, as well as live parameter optimization of digital signal clipping level and individual subcarrier amplitude [22,23].

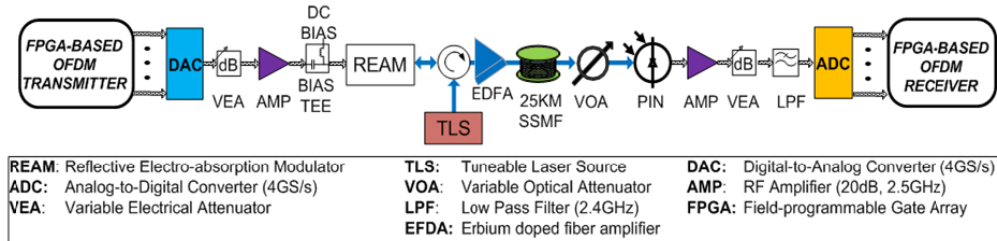| REAM:	Reflective Electro-absorption Modulator	TLS:	Tuneable Laser Source	DAC:	Digital-to-Analog Converter (4GS/s)
ADC:	Analog-to-Digital Converter (4GS/s)	VOA:	Variable Optical Attenuator	AMP:	RF Amplifier (20dB, 2.5GHz)
VEA:	Variable Electrical Attenuator	LPF:	Low Pass Filter (2.4GHz)	FPGA:	Field-programmable Gate Array
		EFDA:	Erbium doped fiber amplifier		

Fig. 1. Experimental system setup for colorless real-time unidirectional OOFDM transmission based on an REAM-IM.

As shown in Fig. 1, at the transmitter side, after passing through an optical circulator with 1.4dB insertion loss, an optical continuous wave (CW) supplied by a tunable laser source (TLS) is injected, at an optical power of 3dBm, into a polarization-insensitive REAM with an electrical modulation bandwidth of ~8GHz. A digital OFDM signal emerging from the FPGA is first converted to an analog signal via the DAC, and the converted electrical signal power level is then optimized by a variable electrical attenuator combined with a 2.5GHz RF amplifier. The resulting 2GHz 1.5Vpp electrical analog OFDM signal and an optimum reverse bias DC voltage are combined in a 50GHz bias tee to modulate the CW optical wave of a specific wavelength in the REAM-IM operating at a temperature of 19.5⌡C. Once the real-time OOFDM signal is generated, an Erbium doped fiber amplifier (EDFA) is utilized to boost the optical signal to 5.84dBm for transmitting through the 5dB-loss 25km SSMF transmission system.

At the receiver side, the optical signal passes through a variable optical attenuator to adjust the ROP and is then directly detected by a 12GHz p-i-n detector to convert the transmitted OOFDM signal into the electrical domain. The received analog OFDM signal is digitized by the 8-bit ADC operating at 4GS/s. By employing real-time DSP procedures detailed in [18–23], all 15 data-carrying subcarriers in the positive frequency bins are used for automatic symbol alignment, channel estimation/equalization and data recovery. In addition, the BER analyzer continuously counts errors for every 88500 symbols, which corresponds to a total test pattern of 6 608 000 bits.

2.2. Measured characterization results

Making use of the OOFDM transceiver design and the experimental system setup described in Section 2.1, optimizations of transceiver and system operating conditions are first conducted in real-time to maximize the obtainable signal line rate by effectively compensating for the system frequency response roll-off effect through adaptive bit and power loading performed at the information-bearing subcarriers [18–23]. Figure 2(a) illustrates the obtained optimum subcarrier bit allocation profile corresponding to a raw signal bit rate of 10Gb/s, of which 8Gb/s can be employed to carry user data because of the use of a 25% cyclic prefix. It can be seen in Fig. 2(a) that lower signal modulation formats occur in the low and several high frequency subcarriers, this is attributed to the combined effects of strong subcarrier intermixing upon direct detection in the receiver and the residual system frequency response roll-off. The first (second) effect is pronounced for subcarriers having low (high) frequencies. In addition, to identify the wavelength-dependant reverse bias DC voltage required by the REAM-IM, optical power loss characteristics of the REAM-IM against reverse bias DC voltage are also measured for various wavelengths within the C-band, the corresponding results are depicted in Fig. 2(b). Throughout the present paper, Fig. 2(b) is used as an important reference for selecting optimum REAM-IM operating conditions.
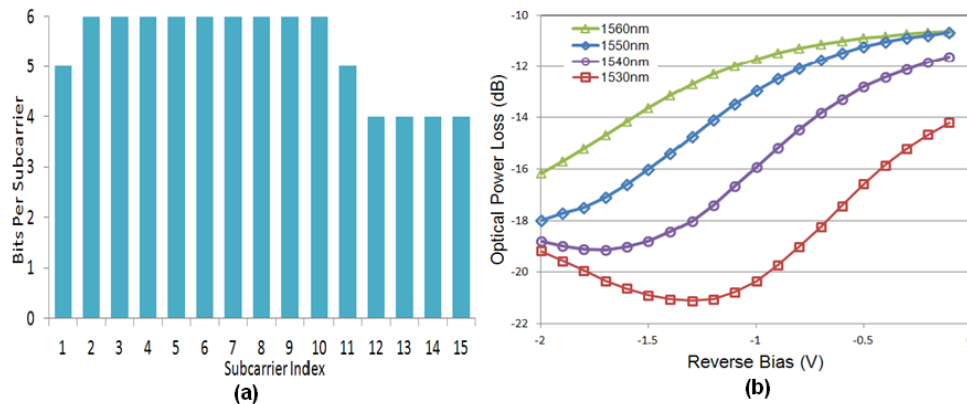

Fig. 2. a) Adaptive bit allocation for the REAM-IM-based OOFDM-PON system and b) Insertion loss of the REAM-IM for different reverse DC bias voltages and operating wavelengths in the C-band for a CW input signal.

The measured system frequency responses for three representative wavelengths across the C-band are shown in Fig. 3(a), in obtaining which experimental measurements are performed from the transmitter IFFT input to the receiver FFT output, and normalization is made to the first subcarrier power. For comparison, the system frequency response reported in [9] for a RSOA-IM-based 25km SSMF OOFDM-PON system is also plotted in Fig. 3(a). It is clearly shown in Fig. 3(a) that, due to an increased modulation bandwidth of the REAM-IM, the maximum roll-off of the REAM-IM-based system frequency response is decreased by approximately 8dB, compared to that corresponding to the RSOA-IM-based system of an identical transmission distance and the same wavelength. As a direct result, the employment of a uniform bit loading profile reported in [9] and adaptive power loading in the REAM-IM-

based IMDD PON system, results in real-time 7.5Gb/s over 25km SSMF OOFDM transmission, which is identical to that achieved in [9]. However, in the present system, the ROP is decreased by 5 dB and simultaneously the minimum received BER is reduced by a factor of 4.2, compared to its system counterpart incorporating the RSOA-IM.

Based on the optimum bit loading profile presented in Fig. 2(a) and adaptive power loading, for various C-band wavelengths, Fig. 3(b) shows the measured BER performance of end-to-end real-time 10Gb/s OOFDM signals over the 25km SSMF IMDD PON system employing the REAM-IM. As expected from Fig. 2(b), for each wavelength considered, online optimizations of transceiver and system operating conditions including the REAM-IM bias and RF driving voltages are performed to minimize the ROP at a fixed total channel BER of 2.2×10^{-3} (FEC limit). For these three wavelengths shown in Fig. 3(b), the reverse DC bias voltages are 1.6V for 1560nm, 1.2V for 1550nm and 0.7V for 1535nm, and the electrical driving voltage is almost wavelength independent and optimized driving voltages of 1.5Vpp are taken throughout the paper. It is shown in Fig. 3(b) that the REAM-IM is capable of supporting virtually wavelength-independent OOFDM transmissions at 10Gb/s over 25km SSMF for optical wavelengths across the entire C-band. Such colorless signal transmissions correspond to ROP variations as small as <0.5dB at the FEC limit and give rise to minimum total channel BERs of $<1.6 \times 10^{-4}$.
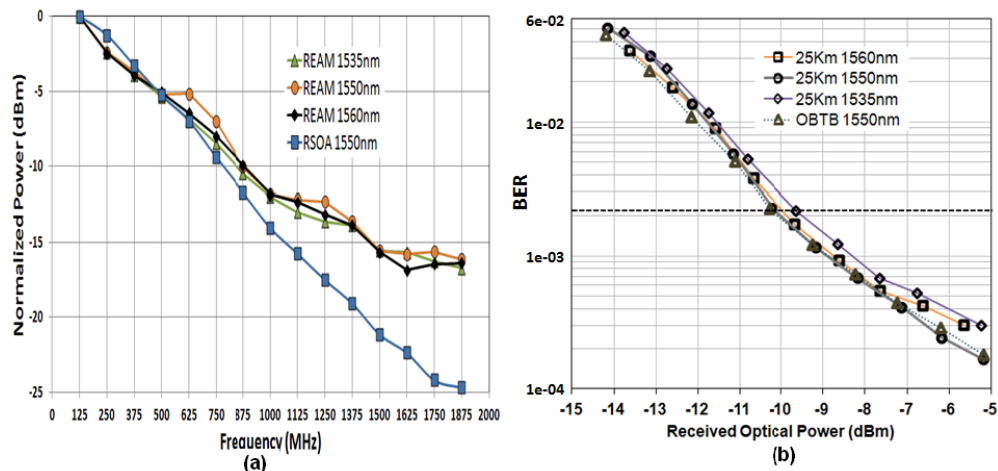

Fig. 3. a) REAM-IM-based and RSOA-IM-based OOFDM-PON system frequency response for different wavelengths. b) REAM-IM-based OOFDM-PON BER performance of the 10Gb/s OOFDM signals for optical back-to-back configuration and 25km SSMF transmission for different wavelengths.

3. 10Gb/s colorless upstream transmission performance of bidirectional REAM-IM-based OOFDM-PONs

3.1. Bidirectional OOFDM-PON

Having undertaken the characterization of colorlessness of the REAM-IM-based unidirectional OOFDM-PON system in Section 2, in this section, detailed experimental investigations are conducted of upstream OOFDM signal transmission over a single-fiber-based, bidirectional OOFDM-PON architecture. For such a case, the RB impairments may significantly affect the performances of both downstream and upstream transmissions. However, in the existing PON wavelength plan, with respect to downstream transmission wavelengths, different wavelengths are widely adopted for upstream transmission, the data-carrying downstream (upstream) transmission-induced RB effect on the data-carrying upstream (downstream) transmission performance is, therefore, negligible. As a direct result, the downstream transmission performance of real-time REAM-IM-modulated OOFDM

signals is very similar to the unidirectional transmission case discussed in Section 2. The main focus of this section is to explore the upstream OOFDM signal transmission performance, which is considerably affected mainly by the downstream transmission of the CW optical signal injected at the OLT. Here it should be noted that, due to the reflective nature of the REAM-IM-based ONU, the downstream propagating RB noise generated by the information-carrying upstream optical signal is amplified by the SOA and subsequently combined with the upstream optical signal after the REAM-IM. The power of such RB noise is proportional to the combined optical gain between the semiconductor optical amplifier (SOA) and the REAM-IM [24].

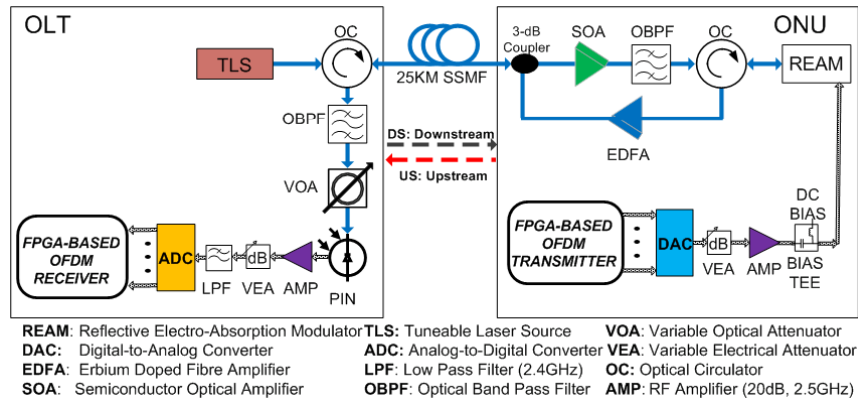| REAM:	Reflective Electro-Absorption Modulator	TLS:	Tuneable Laser Source	VOA:	Variable Optical Attenuator
DAC:	Digital-to-Analog Converter	ADC:	Analog-to-Digital Converter	VEA:	Variable Electrical Attenuator
EDFA:	Erbium Doped Fibre Amplifier	LPF:	Low Pass Filter (2.4GHz)	OC:	Optical Circulator
SOA:	Semiconductor Optical Amplifier	OBPF:	Optical Band Pass Filter	AMP:	RF Amplifier (20dB, 2.5GHz)

Fig. 4. Real-time bidirectional OOFDM-PON for upstream transmission.

Figure 4 shows the real-time bidirectional OOFDM-PON setup utilizing the REAM-IM characterized in Section 2. On the OLT side, after passing through a 1-dB loss optical circulator, an optical CW signal generated by a TLS is launched, with a 2.2dBm optical power, into the 25km 5-dB loss SSMF. On the ONU side, a 3-dB coupler/splitter diverts the CW signal emerging from the 25km SSMF to an SOA followed by a 0.8-nm optical band-pass filter. The SOA biased at 142mA is employed to amplify the attenuated optical CW signal to optimally operate the REAM-IM for minimizing the total channel BER. Once the optical filter removes the out-of-band amplified spontaneous emission (ASE) noise associated by the SOA amplification, and after passing through an 0.8-dB-loss optical circulator, the CW optical signal of a power of 2.3dBm is injected into the REAM-IM. After combined with an optimum reverse bias DC voltage for a given wavelength, a 2GHz 1.5Vpp analogue OFDM signal generated by the DSP processes similar to those presented in Section 2 modulate the CW optical signal in the REAM-IM. After passing again through the ONU-side optical circulator, the intensity-modulated real-time OOFDM signal is directed to an EDFA. Having been amplified and passed through the 3-dB coupler/splitter, the OOFDM signal is injected into the 25km SSMF for upstream transmission. On the OLT side, the optical circulator directs the OOFDM signal to an 0.8nm optical band-pass filter, and then a variable optical attenuator (VOA) for adjusting the ROP for real-time system BER measurements. Finally, the transmitted upstream OOFDM signal is converted to the electrical domain for data recovery utilizing the DSP process described in Section 2.
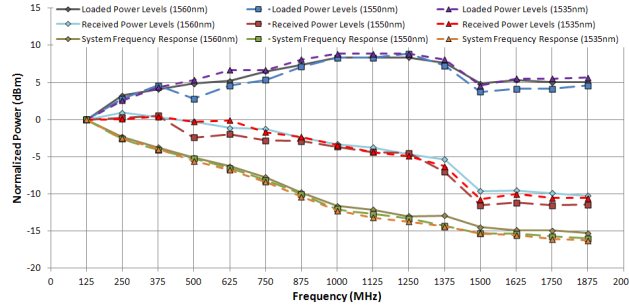
Fig. 5. Adaptively loaded and received subcarrier power profiles and system frequency responses for upstream OOFDM signal transmission in the 25km SSMF bidirectional OOFDM-PON.

3.2. Colorless upstream OOFDM-PON performance

To maximize the upstream signal transmission capacity via effectively compensating for the system frequency response roll-off effect, in addition to the adoption of the adaptive bit loading profile presented in Fig. 2(a), adaptive power loading is also performed on-line for all the information-bearing subcarriers of the upstream OOFDM signal. For different representative wavelengths within the C-band, Fig. 5 shows the loaded subcarrier power profiles and their corresponding received subcarrier power profiles, as well as normalised system frequency responses. Here the identified optimum REAM-IM reverse bias and driving voltages are also employed. As expected, Fig. 5 shows that, for all these wavelengths considered, the maximum upstream system frequency response roll-offs of ~16.25dB are measured, which agree very well with those associated with the unidirectional OOFDM-PON system presented in Fig. 3(a).

Making use of the identified optimum REAM-IM operating conditions, and the optimum bit and power loading profiles shown in Fig. 2(a) and Fig. 5 respectively, Fig. 6 shows the measured total channel BER performance of the 10Gb/s upstream OOFDM signal transmission over the bidirectional PON architecture. As seen in Fig. 6, for all these representative wavelengths across the entire C-band, colorless upstream transmission is achievable with wavelength-dependent ROP variations as small as <0.5dB at the FEC limit. Such slight wavelength-dependent minimum ROP behaviors originate mainly from an optical wavelength-induced variation in extinction ratio of the REAM-IM modulated signal [25]. In addition, optical power budgets of approximately 12.5dB are also measured for all the wavelengths considered. It is expected that the utilization of an optical amplifier before the PIN or other techniques such as wavelength-offset optical filtering [26] can considerably increase the optical power budget.

Representative received constellations of different individual subcarriers recorded prior to channel equalization for different wavelengths are plotted in Fig. 7, in which the total channel BERs of 1.38×10^{-3} for 1560nm, 1.51×10^{-3} for 1550nm and 1.74×10^{-3} for 1535nm are measured. For all the constellations, large variations in subcarrier amplitude level are clearly seen, which agree with the behaviors presented in Fig. 5. In addition, these constellations show very little deviations for different wavelengths, this is verified by the small BER differences between different wavelengths, as shown in Fig. 6.
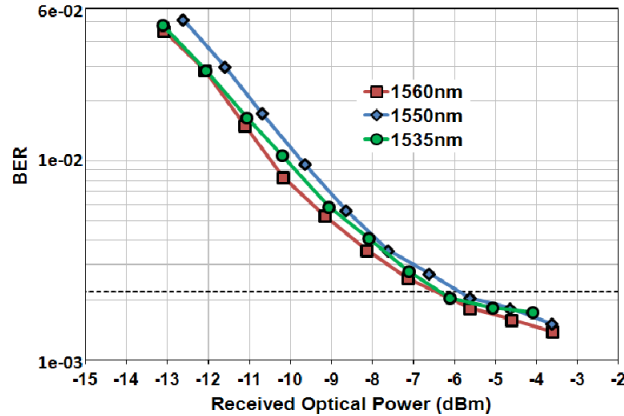
Fig. 6. BER performance of 10Gb/s upstream OOFDM signals for the REAM-IM-based 25km SSMF bidirectional OOFDM-PON for different wavelengths within the C-band.
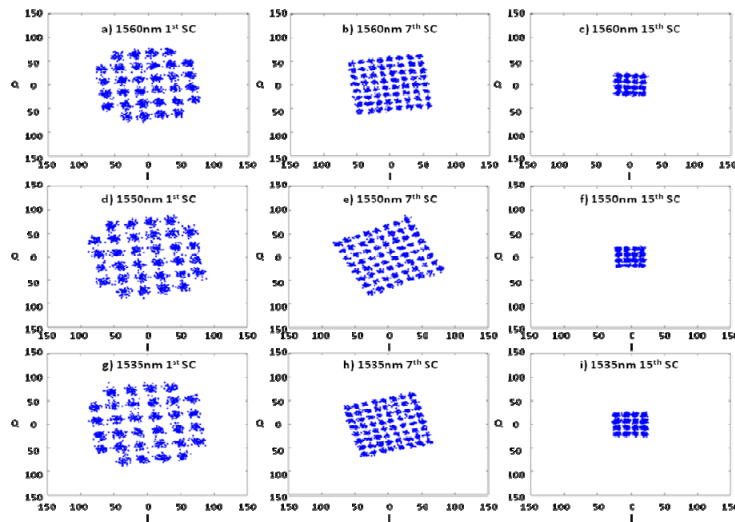

Fig. 7. Received constellations of different subcarriers before channel equalization for the upstream transmission of the 10Gb/s REAM-IM-modulated OOFDM signals over the bidirectional PON. (a)-(c) for 1560nm, (d)-(f) for 1550nm and (g)-(i) for 1535nm.

3.3. RB impact

It is well known that both stimulated Brillion scattering (SBS) and RB can degrade the performance of bidirectional PONs. A typical SBS threshold for a SSMF-based PON system is approximately 7dBm, below which the SBS effect is negligible [24]. As discussed in Section 3.1, in the present OOFDM-PON, the injected optical signal powers for both downstream and upstream transmissions are much lower than the SBS threshold value, indicating that the SBS effect does not play an important role in degrading the PON performance. On the other hand, as also mentioned in Section 3.1, the effect of RB induced by the downstream propagating CW optical signal is, however, unavoidable and appears as random noise added to the upstream OOFDM signal.
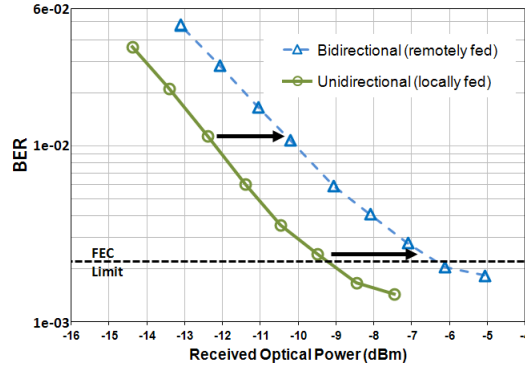
Fig. 8. Impact of RB on the BER performance of upstream 10Gb/s over 25km OOFDM signals.

To explicitly distinguish the impact of RB on the upstream 10Gb/s over 25km SSMF transmission performance of the OOFDM signal, Fig. 8 is plotted, in which comparisons of the total channel BER performances are made between unidirectional and bidirectional cases: in the unidirectional case, a locally-fed CW optical signal is directly injected into the SOA in the ONU side without travelling through the SSMF, and all other components and their operating conditions remain the same as those discussed in Fig. 4 for fair comparison. Whilst in the bidirectional case, the considered OOFDM-PON architecture is identical to that illustrated in Fig. 4. For both cases, the BER performance is measured at an optical wavelength of 1535nm. Clearly, the RB effect exists only in the bidirectional case. It can be seen in Fig. 8 that the impact of RB brings about an approximately 2.8dB optical power penalty at the FEC limit, which is very similar to that reported in [11]. The result suggests that the RB effect is a crucial factor limiting the achievable upstream optical power budget for a given PON architecture. In addition, compared to Fig. 3(b), an increase in minimum achievable BER occurs in Fig. 8 for both cases, this is due to extra ASE noises introduced by optical amplification.

4. Trade-off between signal transmission capacity and optical power budget

From discussions in Sections 2 and 3, it is clear that adaptive bit and power loading provides a simple means of effectively compensating for the system frequency response roll-off effect. Generally speaking, it equips OOFDM-PONs with considerably enhanced flexibility in terms of the achievement of the best overall system performance, which is always maximized according to the actual PON component/system characteristics. As a direct result, the OOFDM-PON with adaptive bit and power loading can be regarded as a versatile function platform capable of satisfying various application scenarios. For example, for a PON system with a fixed optical power budget, the technique enables system designers to maximize the aggregated signal line rate. On the other hand, for a PON system with a specific aggregated signal line rate, the technique allows system designers to maximize the optical power budget. The above analysis raises a very interesting open question, i.e., what is the trade-off between the aggregated signal line rate and corresponding optical power budget for a given PON system. From the practical PON system design point of view, the provision of answers to the open question is of great importance, as the answer can offer a cost-effective and highly dynamic approach for extensively tailoring PON system parameters to the needs of end-users and/or network service providers. This section is dedicated to address, for the first time, the open question.
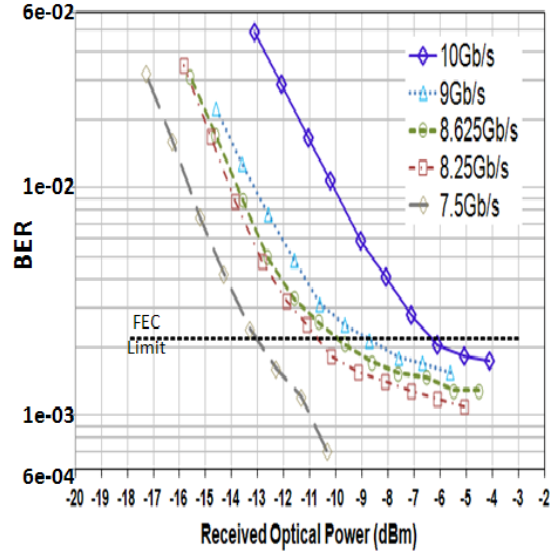
Fig. 9. BER performance of various upstream OOFDM signals over 25km SSMF bidirectional OOFDM-PON.

To experimentally address the aforementioned objective, and to consider the fact that, for a fixed optical launch power, there exists a linear relationship between ROP and optical power budget, the following experimental procedures are adopted in the bidirectional OOFDM-PON shown in Fig. 4:

- Firstly the ROP is fixed at a specific value, and then full use is made of on-line adaptive bit and power loading to ensure that a maximum signal line rate is obtained, corresponding to which the total channel BER at the selected ROP is smaller than the FEC limit;

- For the resulting signal line rate, full BER performance is measured as a function of ROP;

- The above procedure is repeated for a newly selected ROP.

Figure 9 presents the measured BER performances for upstream signal line rates of 10Gb/s, 9Gb/s, 8.625Gb/s, 8.25Gb/s and 7.5Gb/s, whose adaptive bit loading profiles are also given in Fig. 10. In conducting these measurements, optical wavelengths are fixed at 1535nm.
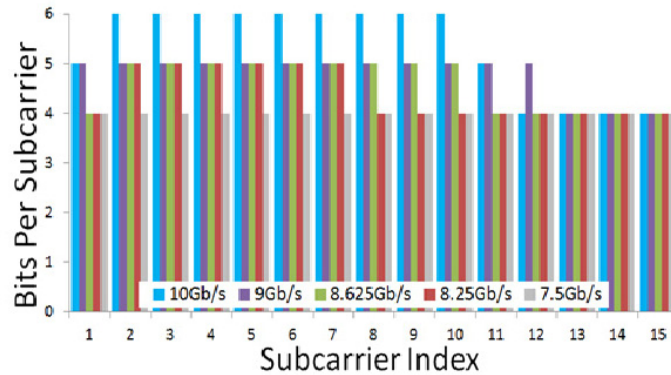

Fig. 10. Adaptive bit loading profiles for different upstream signal line rates achieved in the bidirectional OOFDM-PON.

According to the well-known Shannon's law, it is easy to understand that, for a specific transmission system, there exists a linear relationship between ROP (in dBm) and signal line rate. Making use of Fig. 9, such trade-off is experimentally verified and plotted in Fig. 11. Figure 11 indicates that, for the present PON system, a 10% increase in signal line rate increases the ROP (reduces the optical power budget) by approximately 2.6dB. The slope of such a linear developing trend is mainly attributed to the system bandwidth: a low system bandwidth gives rise to a flat slope, thus causing that a relatively small reduction in signal line rate leads to a relatively large increase in optical power budget. Such a linear relationship between ROP (in dBm) and signal line rate holds well for both SSMF- and multi-mode fiber (MMF)-based transmission systems.
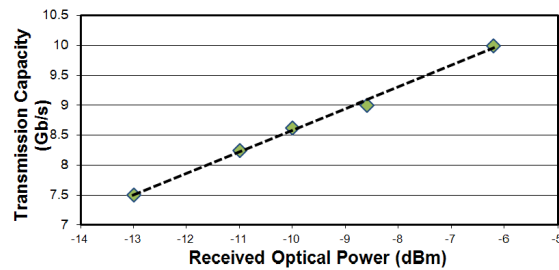

Fig. 11. Measured trade-off between ROP and signal line rate in bidirectional OOFDM-PON.

5. Conclusions

REAM-IMs have been utilized, for the first time, to experimentally demonstrate colorless ONUs in single-fiber-based, bidirectional, IMDD OOFDM-PONs incorporating 25km SSMFs and OLT-side-seeded CW optical signals. Extensive experimental explorations of the PON performance have been undertaken in terms of REAM-IM colorlessness, maximum achievable upstream transmission capacity, key physical factors limiting the upstream OOFDM transmission performance and trade-off between aggregated signal transmission capacity and ROP. Firstly the colorlessness of the REAM-IMs has been characterized, based on which optimum REAM-IM operating conditions are identified. In the aforementioned PON architecture, 10Gb/s upstream colorless transmissions of end-to-end real-time OOFDM signals have been successfully achieved for various wavelengths within the entire C-band. Over such a wavelength window, minimum ROPs at the FEC limit vary in a range as small as <0.5dB. In addition, experimental measurements have also indicated that the RB effect imposes a 2.8dB optical power penalty on the 10Gb/s over 25km upstream OOFDM signal transmission. Furthermore, making use of on-line adaptive bit and power loading, a linear trade-off between aggregated signal line rate and optical power budget (in dB) has been observed, which shows that, for the present PON system, a 10% reduction in signal line rate can improve the optical power budget by 2.6dB. This work has demonstrated the potential of employing REAM-IM-based OOFDM ONUs for NG-PONs.